Progress In Electromagnetics Research Letters, Vol. 109, 65–73, 2023

Single-Fed Wide-Beamwidth Circularly Polarized Antenna Using Reflector-Loaded Bent Dielectric Resonator

Tielin Zhang, Hongmei Liu*, Shaojun Fang, and Zhongbao Wang

Abstract—In the paper, a compact single-fed wide-beamwidth circularly polarized (CP) antenna is proposed. The main radiator of the antenna is a bent dielectric resonator (DR), which is conformal to a rectangle substrate with the same curvature and is excited through a crossed-two-ring slotted ground fed by a T-shaped feeding line. By bending the DR to different curvatures, the half-power bandwidth (HPBW) of the dielectric resonator antenna (DRA) can be adjusted. Besides, to improve the 3-dB axial ratio (AR) beamwidth, as well as further enhance the HPBW, a copper reflector is inserted below the DRA. A prototype operating in BeiDou Navigation Satellite System (BDS) B1 band (1.561 GHz) was designed, and measurement was done to verify the simulations. Measurement results show that from 1.55 GHz to 1.58 GHz, the return loss is more than 10 dB, and the AR is less than 3 dB. At 1.561 GHz, the measured 3-dB AR beamwidths are 165° and 210° at *xoz* and *yoz* planes, respectively, while the HPBWs are 143° and 154° at the two planes.

1. INTRODUCTION

Circularly polarized (CP) antennas, which demonstrate the merits of reducing the multipath effect and polarization mismatch compared with linearly polarized (LP) antennas, have been widely applied in satellite communication, wireless power transmission, global positioning system (GPS), and BeiDou Navigation Satellite System (BDS) [1–3]. In recent years, there is a preference for CP antennas that provide wide 3-dB axial ratio (AR) beamwidth and wide half-power beamwidth (HPBW). The receiving of wireless signals can be ensured by CP antennas with wide 3-dB AR beamwidth no matter whether the satellites are in low or high elevations, while CP antennas with wide HPBW can improve the coverage area and stabilize the received signal, especially in the swayed applications, such as maritime navigation.

The effective techniques for improving AR beamwidth include cavity-backed reflector [4, 5], metasurface [6], annular metal strip loading [7, 8], and inserting slots [9, 10]. In [4, 5], the 3-dB AR beamwidths of the CP antennas reach more than 200° and 240°, respectively, by using the cavity-backed reflector. In [6], the 3-dB AR beamwidth of more than 200° is achieved by loading the metasurface. However, large dimension will be induced by the cavity and metasurface. For size reduction, an annular metal strip is loaded and combined with edge resistors [7] and metal branches [8] for AR beamwidth enhancement. The obtained 3-dB AR beamwidths are more than 180° and 240°, respectively. In [9] and [10], by etching two pairs of asymmetric slots on the patch, 3-dB AR beamwidths of more than 180° are achieved with compact size. Other methods, such as loading pins [11] and dielectric lens [12], can also increase the AR beamwidth. However, the AR beamwidths are limited by the ground plane dimensions.

The methods for HPBW enhancement can be classified into three, including metal walls [13], parasitic radiators [14, 15], and meta-columns [16]. In [13], two diagonal metal walls are adopted for a wide HPBW of more than 100°. In [14], a parasitic ring is loaded above the main radiator to achieve

Received 28 November 2022, Accepted 16 February 2023, Scheduled 1 March 2023
* Corresponding author: Hongmei Liu (lhm323@dlmu.edu.cn).
The authors are with the School of Information Science and Technology, Dalian Maritime University, Dalian, Liaoning 116026, China.

a wide HPBW of 140°. On the basis, dual parasitic radiators are adopted for HPBW enhancement at dual bands [15]. In [16], twelve meta-columns are placed around the main radiator for a wide HPBW of 108°.

However, most of the previous researches only focus on one of the two indexes of AR beamwidth and HPBW. A few methods are reported to simultaneously enhance the 3-dB AR beamwidth and HPBW. In [17], a partially etched superstrate and a conducting cavity are utilized for broadening the 3-dB AR beamwidth (> 160°) and HPBW (> 100°). In [18], circular metal strips are used for wide 3-dB AR beamwidths (186°/163°) and wide HPBWs (126°/120°) at dual bands. Circular dipoles, curved ground planes and corrugated back cavity are deployed in [19] for obtaining a wide 3-dB AR beamwidth of over 230° and a wide HPBW of 150°. However, since feed-networks are required in [18] and [19] for providing quadrature excitations, the structure is complicate. In [20], a wide-beamwidth antenna consisting of parasitic strips and RIS reflector is proposed, which achieves a 3-dB AR beamwidth of more than 180° and an HPBW of 147°. Dielectric lens with stacked cone-shaped cavity [21] can be used for achieving a wide HPBW of 170° with a maintained 3-dB AR beamwidth of more than 200°. However, the dimensions for the two antennas [20, 21] are large.

In the paper, a single-fed CP antenna based on reflector-loaded bent dielectric resonator (DR) is proposed with the features of wide 3-dB AR beamwidth and HPBW. By bending the DR to different curvatures, the HPBW can be widened. Besides, to improve the 3-dB AR beamwidth, as well as further enhance the HPBW, a copper reflector is inserted below the DR. Measurement results demonstrate that at 1.561 GHz, the measured 3-dB AR beamwidths are 165° and 210° in *xoz* and *yoz* planes, respectively, while the HPBWs are 143° and 154° in the two planes. The rest of the paper is organized as follows. Section 2 presents the antenna configuration and evolutions. Section 3 demonstrates the measurements, followed by a conclusion in Section 4.

2. ANTENNA CONFIGURATION AND EVOLUTIONS

The configuration of the proposed CP dielectric resonator antenna (DRA) with wide beamwidth is shown in Fig. 1. Table 1 shows the detailed dimensions. The bent DR ($\varepsilon_r = 10$) which has the dimension of $a \times b \times d$ is served as the radiator and is conformal on a bent F4B substrate ($\varepsilon_r = 3.5$, $h = 0.2$ mm) with the dimension of $g_w \times g_l$. By bending the DR, the HPBW of the antenna can be broadened. A T-shaped transmission line is used for the feeding through the crossed two-ring-slotted ground. The dimensions of the feeding line are $w_{m1} \times l_{m1}$, $w_m \times (l_{l1} + l_{l2})$, and $w_{m2} \times l_{m2}$, sequentially. In order to achieve good CP characteristics, a sector ring with an arc of θ is truncated in the inner ring, and

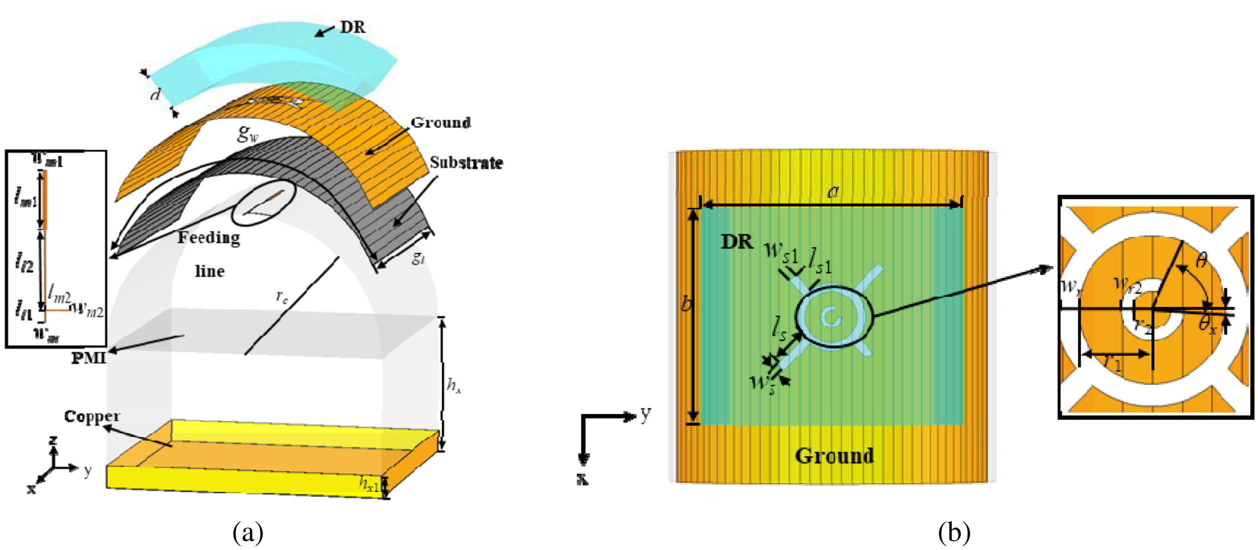

Figure 1. Configuration of the proposed CP DRA. (a) Exploded view. (b) Top view.

Table 1. Dimensions of the proposed antenna (unit: mm).

a	63.6	w_m	0.5	w_r	2.4	r_c	50
b	64.9	l_{l1}	5.4	w_{r2}	1.3	h_x	50
d	14.1	l_{l2}	34.1	w_s	2.4	θ	80°
g_w	120	w_{m2}	0.6	w_{s1}	2.6	θ_x	4°
g_l	100	l_{m2}	9.7	l_s	11.5		
w_{m1}	1.4	r_1	7.8	l_{s1}	6.4		
l_{m1}	25.6	r_2	2.3	h_{x1}	8		

two pairs of crossed bent rectangles are slotted on the ground. The diameters of the inner and outer rings are r_2 and r_1, respectively, while the widths are w_{r2} and w_r, respectively. The dimensions of the two pair bent slotted rectangles are $w_s \times l_s$ and $w_{s1} \times l_{s1}$, respectively. It is noted that the feeding line and slots are placed in the center of the upper and lower surfaces of the substrate, respectively. As the supporter, a semicylinder ($r_c \times g_l$) and a rectangle ($2r_c \times g_l \times h_x$) polymethacrylimide (PMI) material ($\varepsilon_r = 1.05$, $\tan\delta = 0.00028$) are used. To improve the AR beamwidth, as well as further enhance the HPBW, a copper reflector with the height of h_{x1} is inserted under the rectangle PMI.

In the following, the evolutions of the proposed CP DRA are described in detail. The performances of each structure are simulated using HFSS. Firstly, a planar CP DRA (named as Ant. 1) is designed at 1.561 GHz, as shown in Fig. 2(a). Fig. 3 shows the performance of Ant. 1, which exhibits the 10-dB impedance bandwidth (IBW) of 12.66% (1.48 GHz–1.68 GHz), the 3-dB AR beamwidths of 136.43°/152.12°, and the HPBWs of 95.36°/85.42°. To broaden HPBW, the DRA is bent (named as Ant. 2) and conformal on the semicylinder PMI, as shown in Fig. 2(b). As shown in Figs. 3(b) and (c), the HPBW at xoz plane is increased to 122.11°, and the value reaches 145.79° in yoz plane. After bending, the IBW is improved to 19.68% (1.42 GHz–1.73 GHz). However, the 3-dB AR beamwidth is slightly narrowed by the bending. To enhance the 3-dB AR beamwidth, as well as increase the HPBW further, a copper reflector is inserted under CP DRA (named as Ant. 3). Since a distance of approximately $0.5\lambda_0$ is needed between the antenna and the reflector, a rectangle PMI is added above the copper reflector. It is observed from Fig. 3 that the 3-dB AR beamwidths are increased to 167.30° (xoz plane) and 216.87° (yoz plane), while the HPBWs are 156.82° (xoz plane) and 156.65° (yoz plane). Compared with Ant. 1, the 3-dB AR beamwidth is enhanced by 30° and 64° in xoz and yoz planes, respectively. The increments for HPBWs are 61° (xoz plane) and 71° (yoz plane), respectively.

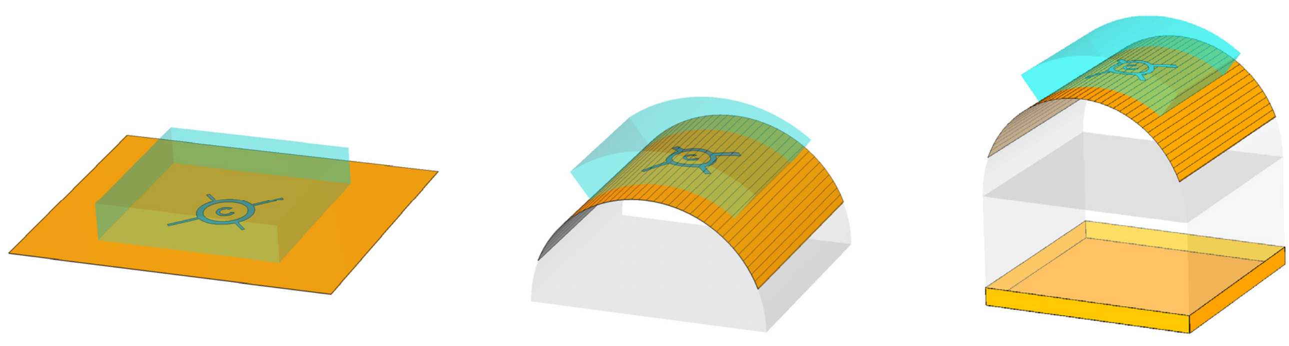

(a) (b) (c)

Figure 2. Evolutions of the proposed CP DRA. (a) Ant. 1. (b) Ant. 2. (c) Ant. 3.

In the evolutions, it is demonstrated that the AR beamwidth and HPBW are affected by the bending of the DR and copper reflector. In this section, a parametric study is presented to illustrate the effects. As the radius of the semicylinder r_c denotes the bending degree, Fig. 4 shows the simulated AR

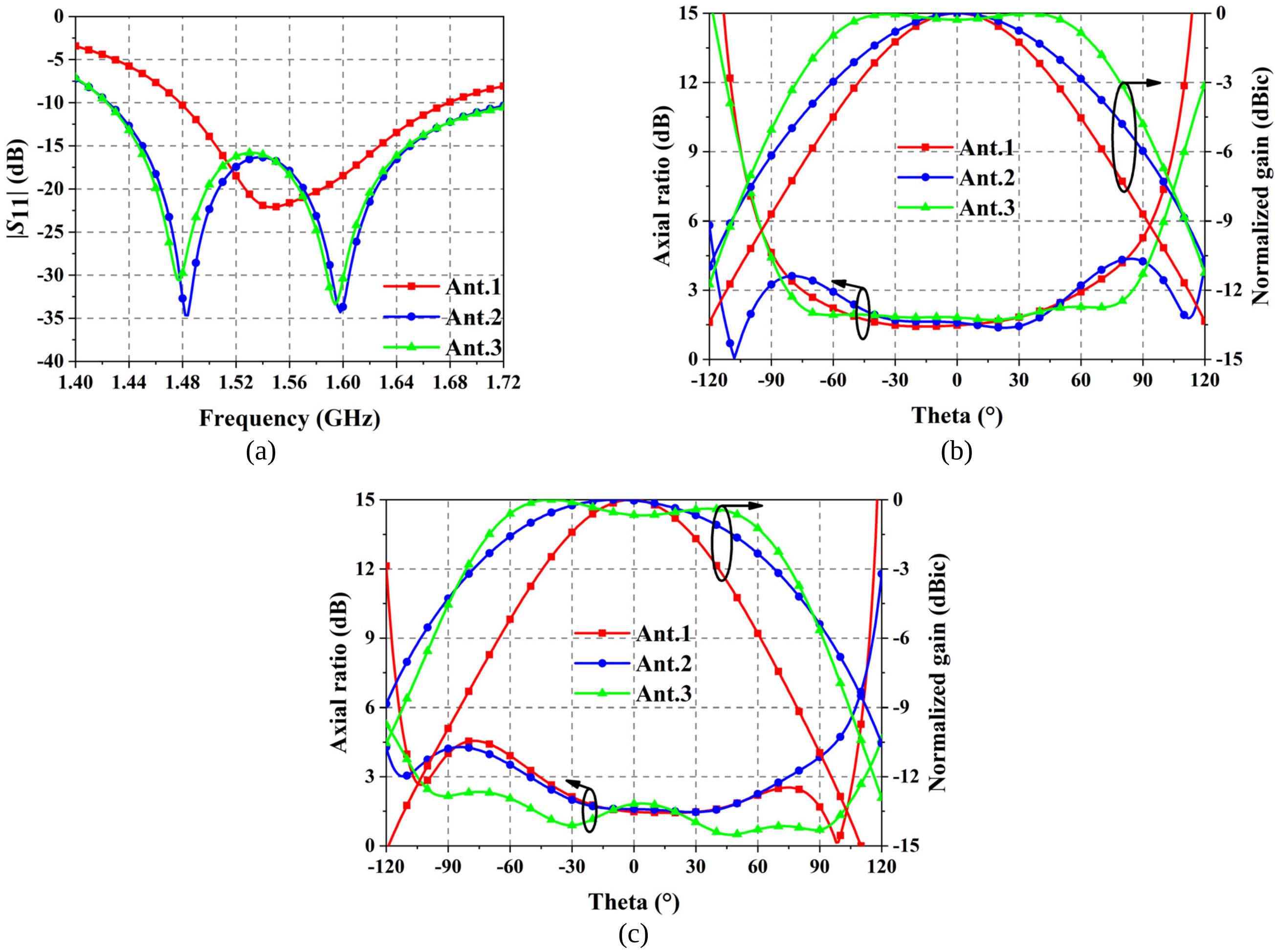

Figure 3. Performance comparisons for different evolutions. (a) $|S_{11}|$. (b) Radiations in *xoz* plane. (c) Radiations in *yoz* plane.

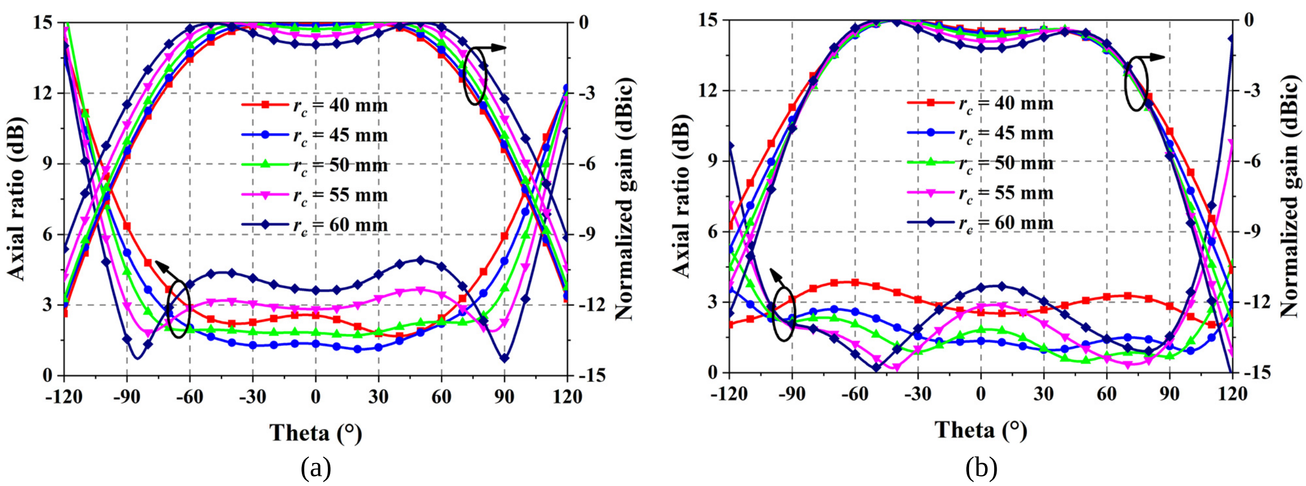

Figure 4. AR and normalized gain for different r_c. (a) *xoz* plane. (b) *yoz* plane.

and normalized gain with different r_c. As observed in Fig. 4(a), the 3-dB AR beamwidth in *xoz* plane is increased from 128.98° to 167.30° when r_c rises from 40 mm to 50 mm. When r_c exceeds 50 mm, most of the AR values are larger than 3 dB. For HPBWs, an increment from 147.85° to 175.47° is observed when r_c changes from 40 mm to 60 mm. At the point for the largest 3-dB AR beamwidth ($r_c = 50$ mm), the HPBW is 156.82°. In the *yoz* plane (see Fig. 4(b)), the 3-dB AR beamwidths for r_c equal to 40 mm, 45 mm, and 50 mm are 73.07°, 231.51°, and 216.87°, respectively. The corresponding HPBWs are 162.94°, 158.19°, and 156.65°, respectively. In consideration of wide 3-dB AR beamwidth and wide HPBW, the value of r_c is determined as 50 mm.

Figure 5 shows the simulated AR and normalized gain with different h_x. It is seen that as h_x increases from 40 mm to 55 mm, the 3-dB AR beamwidths in *xoz* plane are increased from 149.41° to 176.02°, and the HPBWs are raised from 141.47° to 164.55°. The case for $h_x = 60$ mm is ignored since the AR is nearly larger than 3 dB. It is observed in Fig. 5(b) that in *yoz* plane, the 3-dB AR beamwidths for an increasing h_x is around 210°. Although the 3-dB AR beamwidths are similar, the AR values at $\theta = -30° \sim 30°$ are increased with the increase of h_x. The HPBWs in *yoz* plane for $h_x = 40$ mm, 45 mm, 50 mm, and 55 mm are 150.14°, 153.61°, 156.65°, and 160.32°, respectively. Here, the value of h_x is chosen as 50 mm in consideration of the 3-dB AR beamwidth and the flatness of the AR curve.

Besides, the effects of the reflector height (h_{x1}) are also investigated. As demonstrated in Fig. 6, the

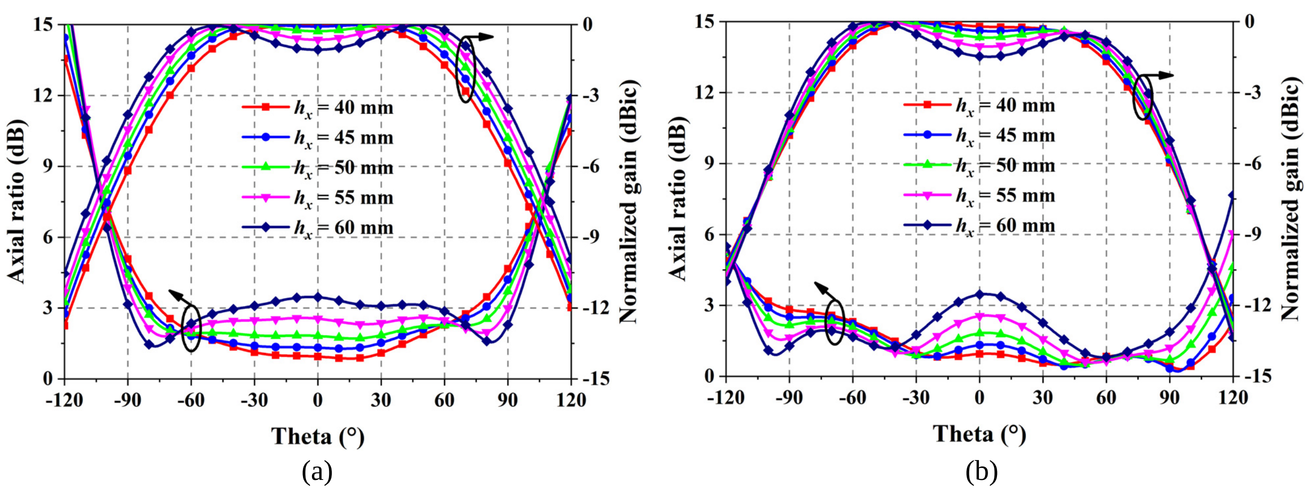

Figure 5. AR and normalized gain for different h_x. (a) *xoz* plane. (b) *yoz* plane.

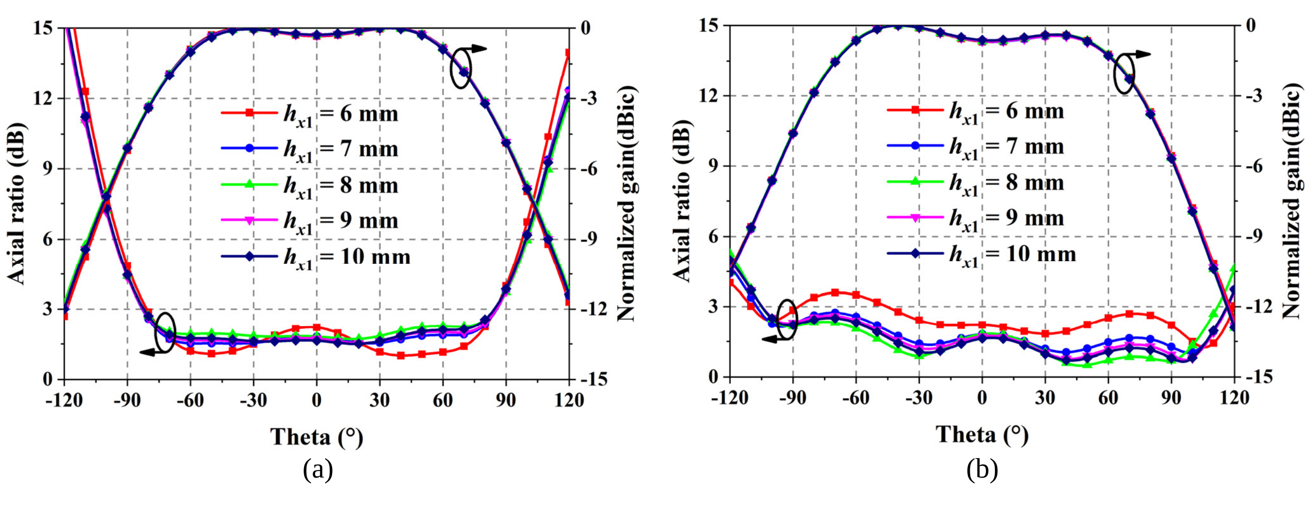

Figure 6. AR and normalized gain for different h_{x1}. (a) *xoz* plane. (b) *yoz* plane.

change of h_{x1} has small influence on the HPBW of the antenna, but affects the AR beamwidth to some extent. As h_{x1} increases, the volatility of AR curve is increased over the whole 3 dB AR beamwidth range. Besides, when h_{x1} is 6 mm, the 3-dB AR beamwidth in yoz plane is narrowed from about 216° to 165.29°. Since the AR curves in the xoz plane are less varied when h_{x1} is larger than 7 mm, the value of h_{x1} is chosen as 8 mm for obtaining lower AR performance in the yoz plane.

3. FABRICATION AND EXPERIMENTAL RESULTS

The designed single-fed CP DRA is fabricated, as shown in Fig. 7. The S-parameters are measured with an Agilent N5230A network analyzer, and the far-field features are measured in an anechoic chamber. Fig. 8 shows the comparisons of simulated and measured results including $|S_{11}|$, AR, and gain. From 1.44 GHz to 1.7 GHz, the measured return loss is larger than 10 dB. From 1.55 GHz to 1.58 GHz, the measured AR and gain are less than 3 dB and more than 2.6 dBic, respectively.

(a) (b)

Figure 7. Photograph of the designed DRA. (a) 3D view. (b) Side view.

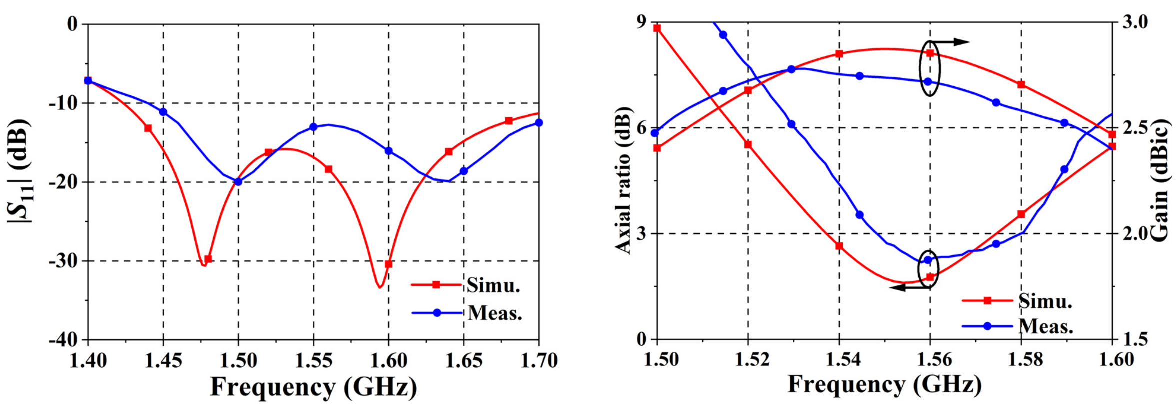

(a) (b)

Figure 8. Simulated and measured results. (a) $|S_{11}|$. (b) ARBW and gain.

Figure 9 depicts the simulated and measured radiation patterns of the designed prototype at 1.561 GHz. The measurements agree reasonably well with the simulations. It is found that in both planes, the right-hand circularly polarized (RHCP) is greater than the left-hand circularly polarized (LHCP). This design also offers a sufficient amount of cross polarization discrimination (> 17 dB) between the RHCP and LHCP in both planes, which is suitable for wide-beamwidth CP antenna applications. Fig. 10 shows the AR and gain curves versus the angle θ. The measured 3-dB AR beamwidths are 165° and 210° in xoz and yoz planes, respectively, while the HPBWs reach 143° and 154° in the two planes.

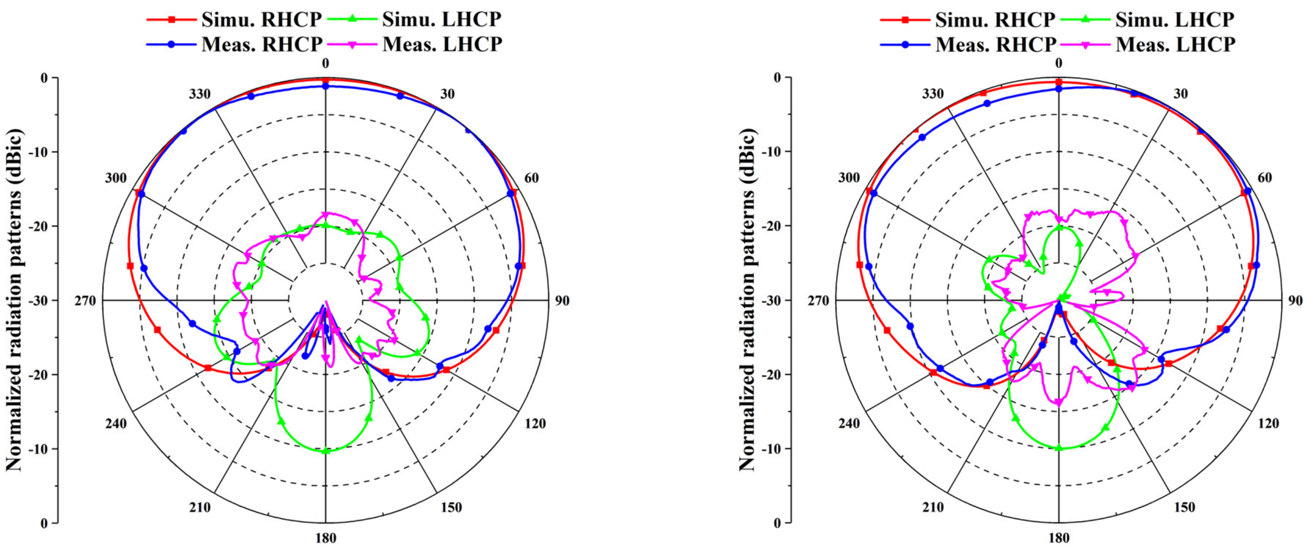

(a) (b)

Figure 9. Radiation patterns of simulation and measurement at 1.561 GHz. (a) *xoz* plane. (b) *yoz* plane.

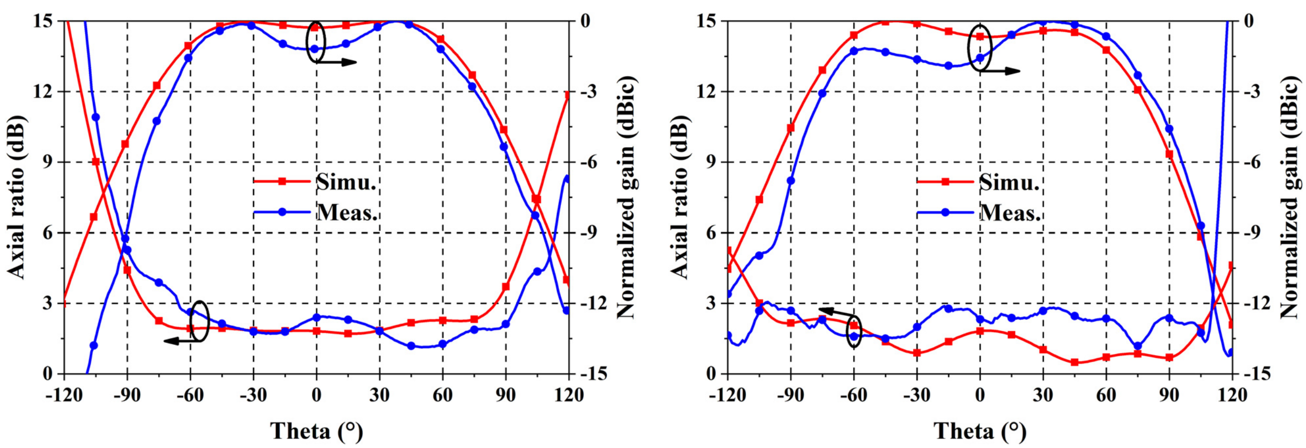

(a) (b)

Figure 10. AR and normalized gain at 1.561 GHz. (a) *xoz* plane. (b) *yoz* plane.

Table 2 illustrates the performance comparisons between the proposed DRA and reported wide-beamwidth CP antennas. In [8] and [14], the performances of 3-dB AR beamwidth and HPBW are widened, respectively. Compare with the works in [17] and [18] where the performances of 3-dB AR beamwidth and HPBW are both improved, the designed antenna shows wider 3-dB AR beamwidth and HPBW. Compared with the work in [19–21] which also own both wide 3-dB AR beamwidth and HPBW, the size of proposed structure is smaller than the work in [20] and [21], while the number of feed points is less than the work in [19] and [21]. In a comprehensive view, the proposed CP DRA exhibits wide 3-dB AR beamwidth, wide HPBW, compact single-fed structure, and small size, which is a good candidate for high-precision BDS applications.

Table 2. Performance comparison between our work and previous wide-beamwidth works.

Ref.	Antenna Technology	Size ($\lambda_0 \times \lambda_0 \times \lambda_0$)	IBW (%)	3-dB AR beamwidth (°)	HPBW (°)	3-dB ARBW (%)	Number of feed point
[8]	Patch with branches	$0.79 \times 0.79 \times 0.14$	25.8	$259^x/238^y$	< 120	5.1	2
[14]	Patch with parasitic ring	$0.56 \times 0.56 \times 0.11$	1.2	Not Given	140^x	0.3	1
[17]	Patch with cavity	$0.30 \times 0.30 \times 0.11$	6.80	$172^x/159^y$	$109^x/103^y$	3.04	1
[18]	PQHA	$0.24 \times 0.24 \times 0.07$	44.8	$186^x/187^y$	$128^x/126^y$	12.2	4
				$167^x/163^y$	$122^x/120^y$	5.1	
[19]	Dipole with cavity	$0.47 \times 0.47 \times 0.38$	19	236^x	150^x	7.52	2
[20]	Patch with RIS	$1.16 \times 1.16 \times 0.15$	4.82	$195^x/202^y$	$147^x/147^y$	Not Given	1
[21]	Patch with lens	$1.28 \times 1.28 \times 0.19$	18.7	$205^x/203^y$	$173^x/170^y$	15.6	2
This Work	DRA with reflector	$0.52 \times 0.52 \times 0.60$	26.51	$165^x/210^y$	$143^x/154^y$	1.92	1

^{x}: In *xoz* plane; ^{y}: In *yoz* plane. λ_0 is the free-space wavelength at the center frequency.

4. CONCLUSION

In the paper, a single-fed CP antenna based on a reflector-loaded bent DR is proposed with the features of wide 3-dB AR beamwidth and HPBW. By bending the DR, an enhancement of HPBW reaches more than 60°. Besides, the 3-dB AR beamwidth can be improved by inserting a copper reflector. The HPBW can also be further enhanced. Measurement results show that the proposed CP DRA exhibits wide 3-dB AR beamwidth, wide HPBW, compact single-fed structure, and small size, which can be applied in BDS for high-precision positioning.

ACKNOWLEDGMENT

This work was supported in part by the National Natural Science Foundation of China under Grant 51809030 and Grant 61871417, in part by the Natural Science Foundation of Liaoning Province under Grant 2020-MS-127, in part by the Liaoning Revitalization Talents Program under Grant XLYC2007067, in part by the Dalian Youth Science and Technology Star Project under Grant 2020RQ007 and in part by the Fundamental Research Funds for the Central Universities under Grant 3132022245.

REFERENCES

1. Ferrero, F., C. Luxey, G. Jacquemod, and R. Staraj, "Dual-band circularly polarized microstrip antenna for satellite applications," *IEEE Antennas Wireless Propag. Lett.*, Vol. 4, 13–15, 2005.
2. Harouni, Z., L. Cirio, L. Osman, A. Gharsallah, and O. Picon, "A dual circularly polarized 2.45-GHz rectenna for wireless power transmission," *IEEE Antennas Wireless Propag. Lett.*, Vol. 10, 306–309, 2011.
3. Wang, S., X. Zhang, L. Zhu, and W. Wu, "Single-fed wide-beamwidth circularly polarized patch antenna using dual-function 3-D printed substrate," *IEEE Antennas Wireless Propag. Lett.*, Vol. 17, No. 4, 649–653, Apr. 2018.
4. Sun, Y.-X., K. W. Leung, and J. Ren, "Dual-band circularly polarized antenna with wide axial ratio beamwidths for upper hemispherical coverage," *IEEE Access*, Vol. 6, 58132–58138, 2018.
5. Zheng, D., Y. Luo, and Q. Chu, "Cavity-backed self-phased circularly polarized multidipole antenna with wide axial-ratio beamwidth," *IEEE Antennas Wireless Propag. Lett.*, Vol. 16, 1998–2001, 2017.

6. Liu, S., D. Yang, and J. Pan, "A low-profile circularly polarized metasurface antenna with wide axial-ratio beamwidth," *IEEE Antennas Wireless Propag. Lett.*, Vol. 18, No. 7, 1438–1442, Jul. 2019.
7. Liu, H., C. Xun, S.-J. Fang, and Z. Wang, "Compact dual-band circularly polarized patch antenna with wide 3-dB axial ratio beamwidth for BeiDou applications," *Progress In Electromagnetics Research M*, Vol. 87, 103–113, 2019.
8. Liu, H., Y. Zhang, Y. Wang, S. Fang, and Z. Wang, "Circular polarized patch antenna with wide 3-dB axial ratio beamwidth and suppressed backward cross-polarized radiation for high-precision marine navigation applications," *IET Microw. Antennas Propag.*, Vol. 15, No. 11, 1393–1401, Oct. 2021.
9. Wang, M.-S., X.-Q. Zhu, Y.-X. Guo, and W. Wu, "Compact circularly polarized patch antenna with wide axial-ratio beamwidth," *IEEE Antennas Wireless Propag. Lett.*, Vol. 17, No. 4, 714–718, Apr. 2018.
10. Ray, M. K., K. Mandal, and N. Nasimuddin, "Low-profile circularly polarized patch antenna with wide 3 dB beamwidth," *IEEE Antennas Wireless Propag. Lett.*, Vol. 18, No. 12, 2473–2477, Dec. 2019.
11. Zhang, X., L. Zhu, and N. Liu, "Pin-loaded circularly-polarized patch antennas with wide 3-dB axial ratio beamwidth," *IEEE Trans. Antennas Propag.*, Vol. 65, No. 2, 521–528, Feb. 2017.
12. Mu, C., S. Fang, H. Liu, Z. Wang, and S. Fu, "3-D-printed dielectric lens with cone-shaped cavity for axial ratio beamwidth enhancement of circularly polarized patch antenna," *IEEE Access*, Vol. 7, 105062–105071, 2019.
13. He, S. and J. Deng, "Compact and single-feed circularly polarised microstrip antenna with wide beamwidth and axial-ratio beamwidth," *Electron. Lett.*, Vol. 53, No. 15, 1013–1015, Jul. 2017.
14. Pan, Z., W. Lin, and Q. Chu, "Compact wide-beam circularly-polarized microstrip antenna with a parasitic ring for CNSS application," *IEEE Trans. Antennas Propag.*, Vol. 62, No. 5, 2847–2850, May 2014.
15. Liu, H., C. Xun, S. Fang, and Z. Wang, "Beamwidth-enhanced low-profile dual-band circular polarized patch antenna for CNSS applications," *Int. J. Antennas Propag.*, Vol. 2019, Art. no. 7630815, 2019.
16. Feng, B., L. Li, K. L. Chung, and Y. Li, "Wideband widebeam dual circularly polarized magnetoelectric dipole antenna/array with meta-columns loading for 5G and beyond," *IEEE Trans. Antennas Propag.*, Vol. 69, No. 1, 219–228, Jan. 2021.
17. Ye, X., M. He, P. Zhou, and H. Sun, "A compact single-feed circularly polarized microstrip antenna with symmetric and wide-beamwidth radiation pattern," *Int. J. Antennas Propag.*, Vol. 2013, Art. no. 106516, 2013.
18. Liu, H., M. Shi, S. Fang, and Z. Wang, "Design of low-profile dual-band printed quadrifilar helix antenna with wide beamwidth for UAV GPS applications," *IEEE Access*, Vol. 8, 157541–157548, 2020.
19. Sun, Y., K. W. Leung, and K. Lu, "Broadbeam cross-dipole antenna for GPS applications," *IEEE Trans. Antennas Propag.*, Vol. 65, No. 10, 5605–5610, Oct. 2017.
20. Yuan, Y., M. Wang, Y. Yin, and W. Wu, "Wide-beam circularly polarized microstrip antenna with high front-to-back ratio for CNSS application," *Proc. Sixth Asia-Pacific Conf. Antennas Propag.*, 2017.
21. Liu, H., C. Mu, T. Yan, S. Fang, G. Wang, and Z. Wang, "Dielectric lens with stacked cone-shaped cavity for broadside radiation enhancement of circularly polarized patch antenna," *IET Microw. Antennas Propag.*, 2020.